EfficientXpert: Efficient Domain Adaptation for Large Language Models via Propagation-Aware Pruning

Songlin Zhao¹, Michael Pitts², Zhuwei Qin²

¹University of California Berkeley ²San Francisco State University tagorezhao@berkeley.edu, mpitts1@sfsu.edu, zwqin@sfsu.edu

Abstract

The rapid advancement of large language models (LLMs) has created an increasing demand for domain-specialized variants in areas such as law, healthcare, and finance. However, their large size remains a barrier to deployment in resourceconstrained environments, and existing compression methods either fail to generalize across domains or introduce high overhead. In this work, we propose EfficientXpert, a lightweight domain pruning framework that combines a propagation-aware pruning criterion (Foresight Mask) with an efficient adapter update algorithm (Partial Brain Surgeon). Embedded within the LoRA fine-tuning process, EfficientXpert enables a one-step transformation of general pretrained models into sparse, domain-adapted experts. It achieves up to 98% of original dense model performance at 40% sparsity on tasks in the health and legal domains, outperforming state-of-the-art approaches. Further analysis reveals significant domain-dependent structural shifts that undermine general pruning masks, highlighting the necessity of adaptive, domain-aware pruning strategies tailored to each domain's unique model changes.

Introduction

Domain-specific LLMs have advanced rapidly in recent years, driven by the growing demand for high accuracy and deep contextual understanding in specialized domains such as legal, healthcare, and finance applications (Song et al. 2025; Zheng et al. 2021; Jin et al. 2019). While general-purpose LLMs demonstrate broad capabilities, they often underperform on tasks requiring domain-specific knowledge and reasoning (Romanov and Shivade 2018). To address this gap and efficiently adapt models to domain-specific vocabulary, structure, and inference tasks, Parameter-Efficient Fine-Tuning (PEFT) is frequently employed, achieving performance comparable to full-parameter fine-tuning (Song et al. 2025; Li and Liang 2021).

Among various PEFT methods, Low-Rank Adaptation (LoRA) has become particularly popular due to its ability to achieve strong adaptation by modifying only a small subset of parameters through low-rank updates (Hu et al. 2022). Despite reducing training costs, PEFT-adapted domain-specific LLMs still inherit the large size and inference overhead of their base models, posing significant challenges

Copyright © 2026, Association for the Advancement of Artificial Intelligence (www.aaai.org). All rights reserved.

for deployment in resource-constrained environments. Consequently, there is a critical need to compress domain-specialized LLMs, retaining domain performance while minimizing computational and memory demands (Frantar and Alistarh 2023; Han, Mao, and Dally 2015).

One promising approach to reducing the size of LLMs is model pruning, which eliminates redundant weights to lower memory and computation costs (Han, Mao, and Dally 2015). Recent methods such as SparseGPT (Frantar and Alistarh 2023) and Wanda (Sun et al. 2023) demonstrate that a twostep pipeline, pruning a general model and subsequently applying PEFT, can preserve performance on general-purpose benchmarks, even at high sparsity levels. However, such general-purpose pruning strategies often fail in domainspecific settings due to two key limitations. First, they rely on static pruning masks that fail to reflect the shifts in weight importance and distribution that arise during domain adaptation (Zhang et al. 2024; Bhattacharyya and Kim 2025). Second, PEFT methods like LoRA do not preserve sparsity: reapplying the pruning mask afterward often leads to large performance drops due to misalignment (Zhang et al. 2024; Hu et al. 2022).

To address these challenges, recent methods such as ATP (Lu et al. 2024) and D-Pruner (Zhang et al. 2024) incorporate domain-aware pruning and fine-tuning strategies to bridge this gap. ATP employs a trainable pruning-decision generator, which adaptively refines model structure throughout the LoRA fine-tuning process (Lu et al. 2024). D-Pruner, in contrast, uses a dual-pruning strategy that jointly considers both general and domain-specific weight importance using gradient-based approximations and regularization techniques (Zhang et al. 2024). While effective, their reliance on gradient-based methods with retraining and auxiliary neural networks incurs substantial computational overhead, adding further cost to an already expensive fine-tuning pipeline (Zhang et al. 2024; Lu et al. 2024). Moreover, these prior methods evaluate only a limited set of tasks, whereas our broader evaluation demonstrates that pruning sensitivity depends more critically on domain than task, highlighting a key oversight in earlier approaches.

In this work, we introduce EfficientXpert, a lightweight and efficient framework that unifies pruning and LoRA finetuning to obtain domain-specific LLMs. By explicitly accounting for domain-specific pruning sensitivity, EfficientXpert provides a scalable, low-cost solution ideal for realworld use. It introduces two key innovations:

- Foresight Mask: A domain-aware pruning method that incorporates forward error propagation into its scoring mechanism by estimating the impact of weights on downstream representations. It enables dynamic, gradient-free mask updates during fine-tuning by leveraging both frozen base weights and evolving adapters.
- Partial Brain Surgeon: An efficient adapter realignment step that solves a ridge regression to suppress pruned coordinates, ensuring that low-rank updates stay aligned with the evolving sparse structure.

Together, EfficientXpert integrates both components into the LoRA fine-tuning process, enabling a one-step transformation of a general pretrained model into a sparse domain expert with minimal overhead. Across a comprehensive set of tasks that span the health and legal domains, EfficientXpert achieves up to 99.8% and 98.43% of the dense model's performance at 40% sparsity on LLaMA-7B.

Beyond empirical results, our analysis demonstrates that pruning sensitivity is fundamentally shaped by the domain of adaptation. Some domains exhibit substantial shifts in weight importance and outlier structure, causing strong misalignment with general-purpose pruning masks. Additionally, we find that domain shifts lead to greater divergence in adapter subspaces than task differences. These findings confirm that domain, more than task, drives pruning behavior and highlight the need for domain-adaptive pruning in efficient model specialization.

Related Work

Parameter-Efficient Fine-Tuning

As LLMs grow in size and capability, Parameter-Efficient Fine-Tuning (PEFT) has emerged as a vital strategy for adapting pretrained models to domains and downstream tasks (Li and Liang 2021). Among these, Low-Rank Adaptation (LoRA) has emerged as one of the most widely adopted approaches for adapting LLMs to new domains and tasks.

LoRA injects trainable low-rank matrices into the attention and feedforward layers of transformer models, enabling efficient adaptation while leaving the original weights unchanged (Hu et al. 2022). LoRA's simplicity and strong empirical performance have driven its rapid adoption in domains such as biomedicine, law, and finance, where recent models like FinGPT (Yang, Liu, and Wang 2023), Med-PaLM (Anil et al. 2023), and LawGPT (Zhou et al. 2024) successfully adapt general-purpose LLMs to specialized tasks with limited supervision and compute. Despite its success, LoRA does not reduce the size or latency of the final model, since the frozen backbone remains fully intact. Recent works have begun to explore combinations of LoRA with pruning on general tasks, seeking to preserve LoRA's training efficiency while improving deployment efficiency (Zhang et al. 2023, 2025). However, the mechanisms by which low-rank updates capture domain- and taskspecific information remain largely unexplored.

Neural Network Pruning

Pruning has long been a fundamental approach for compressing neural networks by eliminating weights with minimal impact on task performance. While iterative magnitude-based pruning proved effective in early CNNs (Han, Mao, and Dally 2015; Qin et al. 2018; Park et al. 2020), it becomes impractical for LLMs due to high retraining costs and activation outliers (Sun et al. 2024; An et al. 2025; Kuznedelev et al. 2023; Cheng, Zhang, and Shi 2024).

To address this, general pruning methods like SparseGPT (Frantar and Alistarh 2023) and Wanda (Sun et al. 2023) compress pretrained LLMs by identifying and removing weights that contribute least to performance on general benchmarks. These benchmarks closely resemble the LLM's pretraining distribution, so pruning masks generated from local approximations (e.g., second-order information or activation statistics) align well with the model's weight structure. Consequently, performance can be largely recovered by fine-tuning on similar general-purpose datasets, even at high sparsity levels.

However, domain-specific adaptation fundamentally differs from general fine-tuning because domain datasets typically deviate significantly from the original pretraining distribution (Zhang et al. 2024). When an LLM is fine-tuned for a specialized domain, such as legal or biomedical tasks, it undergoes substantial shifts in weight importance and internal structure due to new terminology, reasoning patterns, or unique data characteristics. Thus, applying pruning masks derived from the general-purpose model (before domain fine-tuning) becomes problematic, as these pruning decisions become misaligned with the new, domain-specific weight distribution. Alternatively, pruning the model after domain fine-tuning can lead to significant performance degradation, necessitating costly additional rounds of finetuning (Lu et al. 2024; Zhang et al. 2024; Wu, Chen, and Wang 2025; Wu et al. 2025; Guo, Gao, and Yuan 2025).

To overcome these limitations, recent works such as ATP and D-Pruner introduce domain adaptive pruning (Lu et al. 2024; Zhang et al. 2024). D-Pruner combines general and domain-specific importance scores using gradient-based approximations, and applies regularization to preserve weights essential for domain performance (Zhang et al. 2024). ATP, on the other hand, employs a trainable neural pruningdecision network to dynamically update masks during LoRA fine-tuning, and incorporates regularization to align lowrank adapters with the evolving sparse structure (Lu et al. 2024). Although effective, both methods incur significant computational overhead due to reliance on gradient-based criteria or training auxiliary neural networks (Zhang et al. 2024; Lu et al. 2024). Moreover, despite their effectiveness, these works have largely overlooked the fundamental question of why general pruning methods fail in domain-specific settings and how factors like domain identity versus task similarity influence pruning sensitivity.

Methodology

EfficientXpert centers on two tightly integrated components. The **ForeSight Mask** dynamically determines domain-

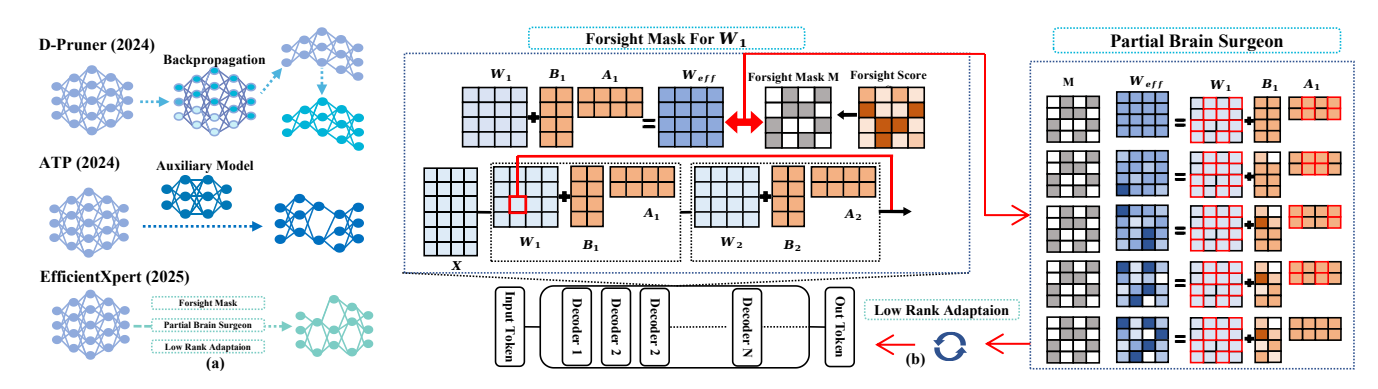


Figure 1: (a) Comparison of EfficientXpert with existing domain pruning methods. (b) Overview of EfficientXpert framework, including ForeSight Mask and Partial Brain Surgeon. EfficientXpert iteratively updates adapters, smooths importance scores, applies corrections to surviving weights, and merges the mask into dense weights to create a sparse, domain-specialized expert.

aware pruning by combining frozen general weights with evolving domain-specific adapters, selecting weights based on their impact on downstream errors without gradients. Complementing this, the Partial Brain Surgeon realigns low-rank adapters to the pruning mask by explicitly adjusting adapter weights, preserving critical learning capacity beyond what gradient descent can achieve. Together, they form an efficient process combining LoRA fine-tuning, propagation-aware pruning, and adapter realignment to produce a sparse model optimized for the target domain (see Figure 1).

Notations

To facilitate a clearer understanding of our method, we begin by establishing the notations. For simplicity, consider two consecutive linear layers within a transformer block of a language model, augmented with a LoRA-style low-rank adapter. Let $W_1 \in \mathbb{R}^{m \times n}$ and $W_2 \in \mathbb{R}^{n \times p}$ denote the frozen base weight matrices of the first and second layers, respectively. Their corresponding low-rank evolving adapters are given by $B_1 \in \mathbb{R}^{m \times r}$, $A_1 \in \mathbb{R}^{r \times n}$ and $B_2 \in \mathbb{R}^{n \times r}$, $A_2 \in \mathbb{R}^{r \times p}$, where $r \ll \min(m, n, p)$ is the shared adapter rank. The input activation matrix is denoted by $X \in \mathbb{R}^{l \times m}$, where $l = b \times s$ corresponds to the total number of tokens in a calibration batch of size b and sequence length s. The effective weights after adaptation are $W_1 + B_1A_1$ and $W_2 + B_2 A_2$, respectively. Throughout our analysis, we ignore bias terms and nonlinearities (e.g., GELU) for clarity and focus on obtaining binary mask M for the first layer.

ForeSight Mask: Propagation-Aware Pruning

Pruning upstream weights can cause errors that propagate through layers and compound their impact, which is especially critical in domain-specific tasks where small early distortions undermine downstream performance. Therefore, it is essential to account for error propagation when making pruning decisions. An illustrative example is provided in the Appendix.

To address this limitation, we propose **ForeSight Loss**, a new pruning criterion that foresees the downstream impact

of pruning decisions through forward composition:

$$||X[M \odot (W_1 + B_1 A_1) - (W_1 + B_1 A_1)](W_2 + B_2 A_2)||_F^2$$
.

The evolving adapters B_1A_1 and B_2A_2 , updated early in domain fine-tuning, encode gradient-driven adaptations that highlight subspaces crucial to the target distribution. Notably, ForeSight Mask leverages this signal without gradient computation, implicitly capturing domain information to guide pruning decisions. Motivated by this idea, we develop a second-order approximation to the loss change by considering the **forward path influence** of each weight on subsequent layers. For a weight (i,j) in the first layer, we define its importance as the product of three terms:

- Its magnitude, which reflects the local perturbation strength;
- The ℓ_2 norm of the j-th row in the subsequent weight matrix, which controls the amplification of the perturbation;
- The ℓ_2 norm of the *i*-th input channel across a calibration dataset, representing how often this weight is activated.

Formally, we define the propagation-aware importance score as:

$$\Delta \mathcal{L}_{ij} \propto |(\mathbf{W}_1 + \mathbf{B}_1 \mathbf{A}_1)_{ij}| \cdot ||(\mathbf{W}_2 + \mathbf{B}_2 \mathbf{A}_2)_{j,:}||_2 \cdot ||\mathbf{X}_{:,i}||_2$$

We compute this score for all weights in W_1 , and obtain the binary mask M by removing the p-th percentile of weights row-wise. This two-layer formulation ensures that the pruning decision for W_1 accounts for its effect on the subsequent layer W_2 , capturing the propagation of error. For details about how attention mechanisms and MLP layers are handled, please refer to the Appendix.

Connections to Optimal Brain Damage Our proposed ForeSight importance score can be derived by estimating the ForeSight loss impact of individual weights using a second-order Taylor expansion, similar builds to the classical pruning framework introduced by *Optimal Brain Damage* (OBD). A mathematical derivation can be found in the Appendix. In comparison to Wanda, which uses the product of weight magnitude and activation norm to estimate importance scores locally within each layer, ForeSight incorporates inter-layer structure by simulating how early-layer

pruning distorts outputs in downstream layers. This makes ForeSight a propagation-aware, second-order extension of both OBD and Wanda, tailored specifically for domain adaptation scenarios where preserving downstream fidelity is critical. Its superior ability to capture domain-specific information compared to Wanda is demonstrated in Experiment .

Partial Brain Surgeon

After applying the ForeSight Mask, the low-rank adapters remain unaware of the pruned weights and may continue updating them. Due to their limited capacity, these adapters struggle to learn sparse correction patterns through gradient descent and often fail to align with the critical pruned subnetwork required for effective domain adaptation.

To address this, we introduce a post-hoc adapter correction step that explicitly suppresses the magnitude of the pruned coordinates in the composed weight $W_1 + B_1 A_1$. Formally, we seek a rank-constrained update ΔB that minimizes the Frobenius norm of the masked positions:

$$\min_{\Delta B} \| (1 - M) \odot (W_1 + (B_1 + \Delta B)A_1) \|_F^2$$
,

where $M \in \{0,1\}^{m \times n}$ is the binary mask.

We solve this optimization row by row. For each row i, let $S_i = \{j \mid M_{ij} = 0\}$ denote the indices of pruned positions. Let $(W_1 + B_1 A_1)_{i,S_i} \in \mathbb{R}^{1 \times |S_i|}$ be the residual over pruned coordinates. Since the adapter rank r is typically smaller than the number of pruned entries $|S_i|$, exact recovery is infeasible, resulting in an over-constrained system that can impair performance if not properly addressed (a detailed discussion is provided in the Appendix). We therefore compute the minimum-norm row update $\Delta b_i \in \mathbb{R}^{1 \times r}$ that approximately nulls these coordinates while controlling deviation via Tikhonov regularization:

$$\min_{\Delta b_i} \| (W_1 + B_1 A_1)_{i,S_i} + \Delta b_i A_{:,S_i} \|_2^2 + \lambda \| \Delta b_i \|_2^2, \quad (3)$$

where $\lambda > 0$ is a regularization parameter.

Problem 3 is a ridge-regression with closed-form solution

$$\Delta b_{i} = -(W + BA)_{i,S_{i}} A_{:,S_{i}}^{\top} (A_{:,S_{i}} A_{:,S_{i}}^{\top} + \lambda I_{r})^{-1}$$

$$(4)$$

Stacking the rows yields $\Delta B = [\Delta b_1^\top \cdots \Delta b_m^\top]^\top$, and we replace $B \leftarrow B + \Delta B$.

The *Partial Brain Surgeon* step suppresses pruned weights with minimal adapter perturbation, ensuring its updates remain aligned with the sparse pattern and enabling more efficient learning within the ForeSight Mask's support.

Crucially, this correction also serves as a better initialization point for subsequent gradient updates. Under sparsity constraints, learning dynamics are highly sensitive to initialization. By steering the adapter toward domain-relevant, unpruned pathways from the outset, Partial Brain Surgeon enables more efficient adaptation and learning on the parts of the model that matter most for the target domain.

EfficientXpert Algorithm

Algorithm 1 summarises *EfficientXpert*. Starting from a pretrained backbone, we fine-tune LoRA adapters on the do-

main corpus $\mathbb D$ while simultaneously pruning with a calibration set $\mathbb D_{\text{cal}}$. At each epoch we (i) update the low-rank adapters, (ii) compute layer-wise ForeSight importance scores, (iii) smooth these scores with an Exponential Moving Average (EMA) so the mask can evolve during training, and (iv) apply a Partial Brain Surgeon (PBS) correction that retargets the adapters to the surviving weights. After the final epoch the learned mask M is merged into the dense weights, yielding a sparse, domain-specialised expert.

Algorithm 1: EfficientXpert

```
1: Input: f(X \mid M, W, B, A), \mathbb{D}, \mathbb{D}_{cal}, s, r, T
 2: Output: f^*
 3: for t = 1 to T do
            update B, A on \mathbb{D}
 4:
 5:
            for layer l do
                 S_t^l \leftarrow \text{ForeSight}(l, t)
S^l \leftarrow \eta S_t^l + (1 - \eta) S_{t-1}^l
 6:
 7:
                 prune top-(1-s) rows of S^l

\Delta B^l \leftarrow \operatorname{PBS}(S^l)
 8:
 9:
10:
                 B^l \leftarrow B^l + \Delta B^l
            end for
11:
12: end for
13: merge BA into W, apply M
14: return f^*(X \mid W \odot M)
```

Time Complexity ForeSight costs $\mathcal{O}(mnr)$, whereas Wanda costs $\mathcal{O}(mn)$; because $r \ll \min(m,n)$ (typically $r \in \{4,\ldots,64\}$), the additional overhead is only a small constant factor. Partial Brain Surgeon (PBS) can be executed in parallel across rows, achieving an effective constant time runtime in practice under sufficient compute resources. Alternatively, it can be run sequentially with $\mathcal{O}(m)$ memory, yielding a time complexity of $\mathcal{O}(mr^3)$; since r is typically small, this memory-efficient approach is practical for deployment in constrained environments. In contrast, ATP and D-Pruner invoke transformer-scale decision networks or full-gradient back-propagation, incurring $\mathcal{O}(Lmn)$ time or worse, where L is the number of transformer layers in the backbone model.

Experiment

Datasets Expanding on previous works(Zhang et al. 2024; Lu et al. 2024), we evaluate **EfficientXpert** in two domains: **Health** and **Legal**. Each domain includes tasks such as language modeling, question answering (QA), natural language inference (NLI), and summarization. For the Health domain, we construct a training set from MedNLI, PubMedQA, and HQS at a ratio of 7:7:1, totaling 15,000 instances with a sequence length of 2048 tokens. For the Legal domain, we use CaseHold, ContractNLI, and BillSum at a 7:6:2 ratio, also totaling 15,000 instances with the same sequence length. Ratios are based on task complexity, data availability, and preliminary validation performance. Dataset details are provided in Appendix. For calibration, Wanda and ForeSight use 128 instances of length 2048 from the C4 dataset to ensure consistency. A discussion on the effect of calibration dataset is provided in the Appendix (Williams and Aletras

Table 1: Evaluation in the **Health** domain. Best scores are **bold**, performance surpassing dense baselines are **starred***.

Methods	Harrison	QA		NLI		HealthQuestion Summarization			Rel.%↑
	Perplexity	MedNLI Acc.	MedNLI F1	PubMedQA Acc.	PubMedQA F1	R1	R2	RL	
			LI	LaMA2-7B (sparsity	0.5)				
Dense + LoRA	5.53	68.05	60.22	73.16	43.98	29.52	10.63	26.77	-
D-Pruner	6.74	61.88	_	_	32.58	36.49	13.71	31.85	94.57
ATP	9.53	70.51	_	_	42.06	29.66	10.36	27.38	81.38
Wanda + LoRA	6.22	64.25	41.46	64.60	47.31*	25.86	15.69	23.19	93.29
ForeSight	6.21	72.86*	54.48	69.65	49.30*	27.81	9.27	25.52	99.41
ForeSight+PBS	6.21	59.70	58.21	66.40	47.22*	27.92	9.38	24.65	94.83
			LI	LaMA2-7B (sparsity	0.4)				
ATP	8.47	71.52	_	_	44.60	31.33	11.15	28.21	85.73
Wanda + LoRA	5.82	66.09	62.18	61.70	44.02*	26.94	9.26	24.16	94.87
ForeSight	5.82	65.21	57.66	71.95	47.84*	29.10	10.04	26.11	99.10
ForeSight+PBS	5.74	74.51*	74.83*	71.95	51.08*	30.93*	11.30*	27.74*	106.6
			LL	aMA3.1-8B (sparsit	y 0.5)				
Dense + LoRA	6.49	68.28	68.17	73.60	52.12	27.98	10.51	25.04	-
ATP	13.94	68.57	_	_	36.72	27.91	9.70	24.71	82.44
Wanda + LoRA	7.93	74.77*	56.36	71.7	50.94	26.4	9.61	23.34	96.07
ForeSight	7.92	76.09*	76.46*	71.95	51.05	27.84	10.13	23.99	103.31
ForeSight+PBS	8.16	57.42	56.34	70.55	49.53	25.80	8.85	22.95	89.40
			LL	aMA3.1-8B (sparsit	y 0.4)				
ATP	12.48	75.32	_	-	43.09	29.86	11.16	27.01	88.62
Wanda + LoRA	7.08	72.66*	54.97	73.85	52.12	26.52	9.95	23.22	96.29
ForeSight	7.08	69.03*	63.63	75*	52.90*	26.32	9.42	23.45	98.06
ForeSight+PBS	7.14	67.88	68.21*	73.92*	52.236*	28.20*	9.90	25.45*	99.80

2023; Bandari et al. 2024; Ji et al. 2024; Mitra, Schwalbe, and Klein 2024).

Model Fine-tuning We select LLaMA2-7B-hf (Touvron et al. 2023) and LLaMA3.1-8B (Dubey et al. 2024) as base models, fine-tuning them using Low-Rank Adaptation (LoRA) with a rank of r=8. LoRA adapters are attached to every weight in the models. Fine-tuning hyperparameters are consistently set as follows: global batch size of 32, training for 3 epochs, learning rate of 1×10^{-4} , momentum of 0.01, and the torch_Adam optimizer. Tokenization remains unchanged from the original Huggingface implementation. All fine-tuning and pruning were conducted on 4 NVIDIA A100 GPUs with 80GB memory, using the Huggingface peft library for LoRA training. Models were loaded and trained in float16 precision, with gradient checkpointing enabled to reduce memory consumption. Both dense and Wanda baseline are finetuned using this setup.

Evaluation Metrics We measure language modeling performance using perplexity computed on 300 paragraphs from InternalMed_Harrison for the Health domain and 300 paragraphs from en_legislation from MultiLegalPile for the Legal domain. For the QA and NLI tasks, we report accuracy and F1 scores specifically on the PubMedQA, CaseHold, MedNLI, and ContractNLI datasets. For summarization tasks, the evaluation involves ROUGE-1, ROUGE-2, and ROUGE-L scores on the HQS and Billsum datasets. Model inference settings remain consistent across evaluations, with top_k=50, top_p=0.9, and temperature=0.9. The final reported metrics are averaged over four separate runs to ensure result robustness. We use the Huggingface datasets

and evaluate libraries to compute ROUGE scores for summarization tasks. A detailed description of the evaluation datasets is provided in the Appendix. To enable a fair comparison with domain pruning methods trained on the same datasets but under different fine-tuning settings, we include a metric of *relative performance*, following the protocol proposed by ATP. This metric quantifies the performance of a pruned fine-tuned model relative to its dense counterpart under an equivalent fine-tuning budget. The relative performance is computed as: Rel. % =

$$\left(\frac{1}{n}\sum_{i=1}^{n}\frac{\operatorname{Acc}_{i}^{\operatorname{pruned}}}{\operatorname{Acc}_{i}^{\operatorname{dense}}}+\frac{1}{n}\sum_{i=1}^{n}\frac{\operatorname{F1}_{i}^{\operatorname{pruned}}}{\operatorname{F1}_{i}^{\operatorname{dense}}}+\frac{1}{3}\sum_{j=1}^{3}\frac{\operatorname{ROUGE}_{j}^{\operatorname{pruned}}}{\operatorname{ROUGE}_{j}^{\operatorname{dense}}}\right)\times$$

100 number of evaluation tasks, and $\mathrm{Acc}_i^{\mathrm{pruned}}$, $\mathrm{Acc}_i^{\mathrm{dense}}$, $\mathrm{F1}_i^{\mathrm{pruned}}$, and $\mathrm{F1}_i^{\mathrm{dense}}$ denote the accuracy and F1 score of the pruned and dense models on task i. The terms $\mathrm{ROUGE}_j^{\mathrm{pruned}}$ and $\mathrm{ROUGE}_j^{\mathrm{dense}}$ correspond to the ROUGE-1, ROUGE-2, and ROUGE. All evaluations are conducted on one NVIDIA A100 GPU with 80GB of memory with model loaded at float 16 precision.

Baselines

We evaluate the effectiveness of the **EfficientXpert** framework by comparing it against representative pruning baselines and conducting an ablation study with and without the Partial Brain Surgeon.

Dense + LoRA We fine-tuned LLaMA2-7B-hf (Touvron et al. 2023) and LLaMA3.1-8B (Dubey et al. 2024) using the above setup to track domain performance without pruning.

Wanda + LoRA In accordance with the original method, we first apply Wanda pruning to the base model and subsequently fine-tune it using LoRA on the domain-specific

Table 2: Evaluation in the **Legal** domain. Best pruned scores are **bold**, performance surpassing dense baselines are **starred***.

Methods	MultiLegalPile	Q	4	NLI		Billsum Summarization			Rel.%↑
	Perplexity	ContractNLI Acc.	ContractNLI F1	CaseHold Acc.	CaseHold F1	R1	R2	RL	
			LLaMA2-7B (s	parsity 0.5)					
Dense + LoRA	3.84	75.84	72.50	70.62	68.19	32.71	13.93	18.30	-
D-Pruner	2.73	_	_	_	27.58	31.00	19.03	25.96	93.53
ATP	3.67	_	_	_	_	43.18	23.12	30.06	81.99
Wanda + LoRA	4.35	53.60	46.73	41.33	41.15	33.31*	11.50	17.79	69.57
ForeSight	4.10	71.37	68.38	63.5	63.46	34.11*	11.94	18.43*	93.65
ForeSight+PBS	4.02	69.61	67.12	63.5	63.49	33.94*	12.04	18.43*	92.86
			LLaMA2-7B (s	parsity 0.4)					
ATP	2.82	_	_	_	_	43.8	23.12	30.06	91.23
Wanda + LoRA	4.09	57.62	49.90	46.12	46.35	35.33*	11.83	18.67*	75.28
ForeSight	3.96	77.4*	74.99*	68.5	68.50	37.65*	13.81	19.94*	100.52
ForeSight+PBS	3.88	74.13	70.35	70.5	70.36*	37.47*	13.61	19.91*	100.96
			LLaMA3.1-8B (s	sparsity 0.5)					
Dense + LoRA	4.44	76.14	74.97	82.5	68.65	33.64	15.58	19.66	_
ATP	4.28	_	_	_	_	43.1	22.6	28.65	82.44
Wanda + LoRA	5.35	50.18	39.60	41.5	41.58	35.05*	12.83	19.11	64.83
ForeSight	5.32	72.37	71.27	67.5	67.06	37.81*	14.62	20.56*	94.73
ForeSight+PBS	5.38	74.38	71.94	68	67.71*	35.03*	13.24	19.52	94.61
			LLaMA3.1-8B (s	sparsity 0.4)					
ATP	4.13	_	_	_	_	45.28	25.45	30.15	88.62
Wanda + LoRA	4.83	59.46	48.30	62.5	62.28	35.54*	14.05	20.16*	81.69
ForeSight	4.85	75.60	74.29	73.15	72.94*	35.38*	14.08	19.86*	98.43
ForeSight+PBS	4.82	77.05*	74.97*	64	63.48	35.77*	14.18	20.23*	94.26

datasets. The domain-specific training datasets, LoRA finetuning configuration, and evaluation metrics strictly follow those described in Section . Since LoRA fine-tuning can overwrite sparsity, we reapply the original pruning mask after fine-tuning to maintain the target sparsity level.

D-Pruner and ATP. We also compare **EfficientXpert** with two state-of-the-art domain pruning methods: D-Pruner (Zhang et al. 2024) and ATP (Lu et al. 2024). Since our evaluation spans a broader range of tasks and datasets than prior work, we report previously published results as-is and compare only relative performance scores, which provide a fair basis for cross-setting comparisons.

Main Results

Health Domain In the health domain, EfficientXpert outperforms existing pruning approaches such as Wanda, ATP, and D-Pruner. At a sparsity level of 0.4, EfficientXpert, when augmented with both the ForeSight Mask and Partial Brain Surgeon (PBS), reaches a relative performance of 106.6% on the LLaMA2-7B model and 99.80% on the LLaMA3.1-8B model—surpassing the dense baseline. Even at a higher sparsity level of 0.5, EfficientXpert with ForeSight alone maintains robust performance, achieving 99.41% (LLaMA2-7B) and 103.31% (LLaMA3.1-8B) relative performance. These results highlight EfficientXpert's capacity to preserve and even enhance domain-relevant capabilities under significant compression (Figure 2 (a)).

Legal Domain Notably, EfficientXpert (with and without PBS) consistently outperforms current domain pruning baselines—ATP and D-Pruner—in terms of relative perfor-

mance across all evaluated sparsity levels and model scales. In addition, EfficientXpert surpasses the general pruning method Wanda in all tasks by a significant margin at all sparsity levels (Figure 2 (b)), demonstrating its superior ability to adapt to domain-specific tasks. In addition, at p=0.4 on LLaMA2-7B, they even surpass dense baseline performance, with ForeSight achieving a relative performance of 100.54%, while ForeSight+PBS reaches 100.96%.

Analysis

The results of the Wanda pruning method reveal a significant domain gap in pruning difficulty, with the health domain exhibiting a relative performance of 93.29%-96% across various tasks at 50% sparsity, while the legal domain performance drops to as low as 64.83%-69.57%. This raises a critical question—why do general-purpose pruning methods like Wanda fail in certain domain-specific settings?

Domain Shift Breaks General Pruning Masks

To better understand this domain-dependent behavior, we apply Wanda at 50% sparsity to single task (QA), domain models: PubMedQA model (health domain) and CaseHold model (legal domain). Detailed training recipe can be found in Appendix. We compare two pruning scenarios: (1) pruning fine-tuned models using a mask generated from its own fine-tuned weights, and (2) pruning fine-tuned models using a mask generated from the *base* LLaMA-7B-hf model.

As shown in Figure 2(b), pruning with Wanda on the fine-tuned PubMedQA model leads to only a 3.3% drop in accuracy, whereas the CaseHold model suffers a significantly larger degradation of 37.4%. When applying the

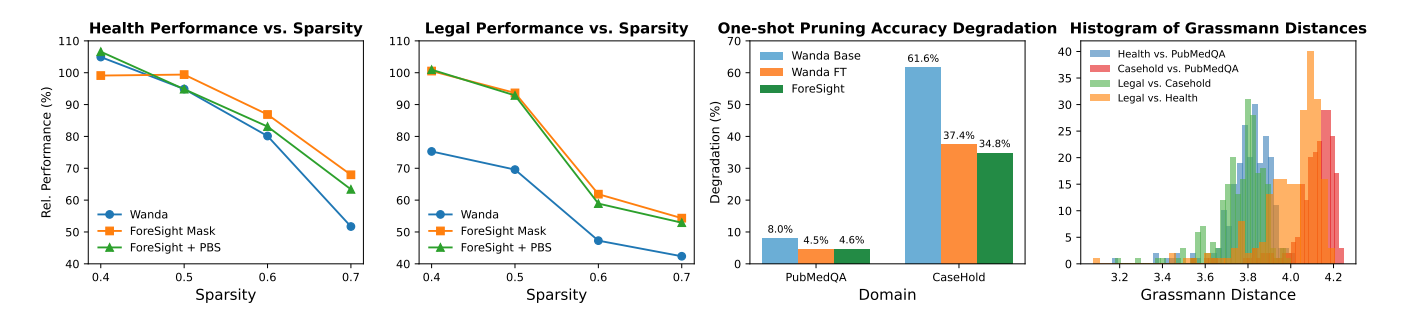


Figure 2: (a) LLaMA2-7B Health Relative Performance vs. Sparsity for different methods. (b) LLaMA2-7B Legal Relative Performance vs. Sparsity for different methods. (c) One-shot Post-Pruning Performance on QA tasks for two domains. (d) Grassmann Distances Analyzing Task Differences vs. Domain Differences.

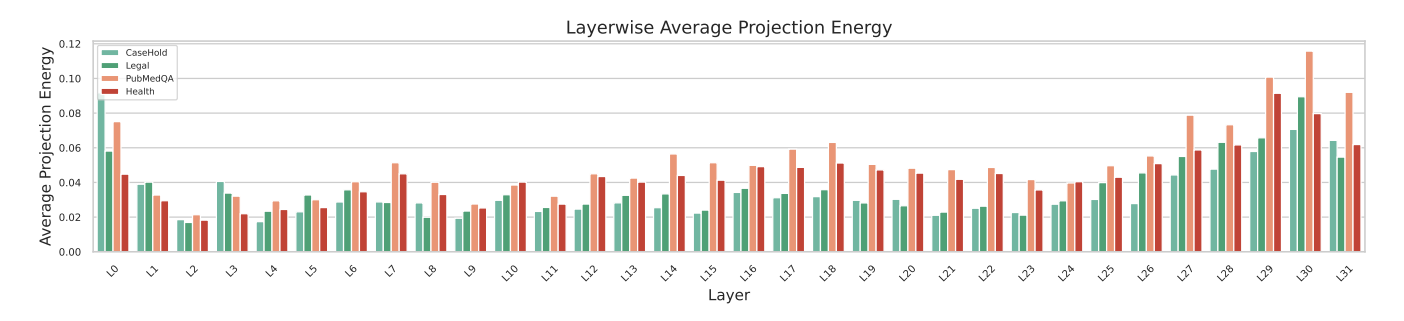


Figure 3: Projection energy across layers.

base-derived mask, the contrast becomes even sharper: Pub-MedQA sees a 5.8% drop, comparable to pruning post fine-tuning, but CaseHold suffers a catastrophic 61.0% drop in performance, far exceeding the already large degradation when pruning was applied after fine-tuning. These results suggest that fine-tuning alters the model's internal structure in domain-specific ways. In CaseHold, fine-tuning appears to substantially shift the distribution of salient weights and activation patterns, making pruning masks generated from the base model highly misaligned and harmful. In contrast, PubMedQA exhibits greater robustness, indicating that fine-tuning induces fewer disruptive changes in weight.

Domains Matter More Than Tasks

Given the significant performance gap we observed when applying general-purpose pruning across domains, a natural question arises: Should pruning strategies group and evaluate models by task type or by domain? To explore this, we first analyze the subspace structure of LoRA adapters by plotting the Grassmann distance distributions between low-rank adapters at each layer for both cross-domain and intradomain model pairs. In addition to the PubMedQA model and CaseHold, we also include task-diverse domain models as controls—specifically, the dense Health and dense Legal models obtained from previous experiments. The computation of Grassmann distance is included in the Appendix.

As shown in Figure 2(c), task-similar but cross-domain adapter pairs (orange: Legal vs. Health; red: CaseHold vs. PubMedQA) exhibit significantly larger Grassmann distances than task-diverse but intra-domain pairs (green: Legal

vs. CaseHold; blue: Health vs. PubMedQA). This indicates that domain identity, more than task type, governs the subspace directions emphasized by fine-tuning.

Next, we compute the projection energy of LoRA adapters onto the top-r singular directions of the pretrained $\|BAV_{W}^{r}(V_{W}^{r})^{\top}\|_{F}^{2}$ $W = U_W \Sigma_W V_W^{\perp}$, The weight matrix. $||BA||_F^2$ score quantifies the proportion of the LoRA adapters that aligns with the top-r right singular vectors of the base weight matrix W. Moreover, Figure 2(d) also shows the average projection energy across all layers, revealing that the intra-domain models (CaseHold and Legal, PubMedQA and Health) exhibit similar trends in projection energy, especially in middle layers (L7 - L25). While the precise mechanisms remain to be fully understood, these findings reinforce the need for domain-aware pruning strategies that account for how fine-tuning reshapes model behavior differently across domains.

Conclusion

We introduce **EfficientXpert**, a domain-aware pruning framework that transforms general-purpose LLMs into sparse, domain-specialized experts with minimal overhead. By integrating the propagation-aware *ForeSight Mask* and the lightweight *Partial Brain Surgeon* update into LoRA fine-tuning, EfficientXpert enables a unified, end-to-end pruning and adaptation process. Our experiments in the health and legal domains show that EfficientXpert consistently outperforms existing pruning baselines across all sparsity levels, achieving performance comparable to the dense

baseline at 40% and 50% sparsity. Our analysis shows that domain-specific adaptation reshapes model subspaces beyond what static, general-purpose pruning captures, highlighting the need for dynamic, domain-sensitive pruning strategies and guiding future sparsity-aware research.

An illustration of error propagation

Illustrative Example. Consider the following matrix multiplication sequence involving two consecutive linear layers:

$$\underbrace{\begin{bmatrix} 3 & 6 \end{bmatrix}}_{X} \cdot \underbrace{\begin{bmatrix} 2 & 2 \\ 4 & 1 \end{bmatrix}}_{W_1} \cdot \underbrace{\begin{bmatrix} 4 & 4 \\ 8 & 1 \end{bmatrix}}_{W_2} = \begin{bmatrix} 192 & 115 \end{bmatrix}.$$

The local loss is defined as $\|X \cdot (M \odot W_1 - W_1)\|_F^2$, and the downstream loss as $\|X \cdot (M \odot W_1 - W_1) \cdot W_2\|_F^2$, where M is the binary mask. Now consider pruning two different weights in W_1 .

Pruning entry $W_{1,1}=2$ (Mask 1) results in a local loss of 36 and a downstream loss of 1152. In contrast, pruning entry $W_{2,2}=1$ (Mask 2) yields the same local loss of 36, but a significantly larger downstream loss of 2340. This toy example illustrates that pruning decisions which are indistinguishable under local error metrics may lead to dramatically different downstream errors due to *error propagation*. As layer depth increases, this effect compounds, motivating the need for pruning strategies that can *foresee* such interactions.

ForeSight for Attention

ForeSight extends to self-attention by pruning the query(Q) and key(K) projections jointly. Throughout, let $X \in \mathbb{R}^{l \times d}$ denote the flattened input activations of a calibration batch $(l = b \times s)$, where b is the batch size and s the per-sample sequence length).

Weights and adapters.

- Base projections: W^Q , $W^K \in \mathbb{R}^{d \times d_k}$ and $W^V \in \mathbb{R}^{d \times d_v}$.
- LoRA adapters: $B^Q, B^K \in \mathbb{R}^{d \times r}, A^Q, A^K \in \mathbb{R}^{r \times d_k}$ and B^V, A^V for the value path.

The effective projections are $\widetilde{W}^Q=W^Q+B^QA^Q$ and $\widetilde{W}^K=W^K+B^KA^K$.

Two-layer interaction. The attention "kernel" observed by the softmax is

$$X \widetilde{W}^Q \widetilde{W}^{K\top} X^{\top}.$$

Masking the Q **projection.** With a binary mask $M^Q \in \{0,1\}^{d \times d_k}$ and sparsity constraint $\|M^Q\|_0 \leq k$, ForeSight selects the k coordinates whose removal minimizes the forward error

$$\min_{M^Q} \left\| X \left[\widetilde{W}^Q - M^Q \odot \widetilde{W}^Q \right] \widetilde{W}^{K \top} \right\|_F^2.$$

A second-order approximation yields the importance score

$$\Delta \mathcal{L}_{ij} \propto \|\widetilde{W}_{ij}^{Q}\| \|\widetilde{W}_{j,:}^{K}\|_{2} \|X_{:,i}\|_{2}.$$

Masking the K **projection.** An analogous problem is solved for $M^K \in \{0, 1\}^{d \times d_k}$:

$$\min_{M^K} \left\| \widetilde{W}^Q \left[\widetilde{W}^K - M^K \odot \widetilde{W}^K \right]^\top X^\top \right\|_F^2, \quad \|M^K\|_0 \le k,$$

with score

$$\Delta \mathcal{L}_{ij} \propto \|\widetilde{W}_{ij}^K\| \|\widetilde{W}_{:,i}^Q\|_2 \|X_{:,i}\|_2.$$

These propagation-aware scores prune Q and K in one pass, ensuring that early-layer sparsity respects downstream attention dynamics.

Derivation of ForeSight importance Score

Let $\mathbf{X} \in \mathbb{R}^{m \times d}$ be a fixed data matrix and let $\mathbf{U}_1 = \mathbf{W}_1 + \mathbf{B}_1 \mathbf{A}_1 \in \mathbb{R}^{d \times h}$, $\mathbf{U}_2 = \mathbf{W}_2 + \mathbf{B}_2 \mathbf{A}_2 \in \mathbb{R}^{h \times p}$ be the (affine, bias-free) effective weight matrices of two consecutive linear layers. Define the loss

$$\mathcal{L}(\mathbf{U}_1) = \|\mathbf{X}\mathbf{U}_1\mathbf{U}_2\|_F^2 = \text{Tr}(\mathbf{U}_2^{\top}\mathbf{U}_1^{\top}\mathbf{X}^{\top}\mathbf{X}\mathbf{U}_1\mathbf{U}_2).$$

Fix an entry $\theta = \mathbf{U}_1[i,j]$. We study the loss change $\Delta \mathcal{L}_{ij}$ obtained by setting this entry to zero while *keeping all other parameters constant*. Throughout we assume (i) \mathbf{X} and \mathbf{U}_2 are constant during the perturbation, (ii) \mathbf{U}_1 corresponds to a first-order stationary point of \mathcal{L} (i.e. $\nabla_{\mathbf{U}_1} \mathcal{L} = \mathbf{0}$), and (iii) higher-than-second-order terms in a Taylor expansion are negligible for the magnitude of the perturbation considered.

Write $E_{ij} = e_i e_j^{\mathsf{T}}$, so that θE_{ij} extracts the affected entry. A standard matrix-calculus identity gives

$$\frac{\partial \mathcal{L}}{\partial \mathbf{U}_1} = 2 \mathbf{X}^{\mathsf{T}} \mathbf{X} \mathbf{U}_1 (\mathbf{U}_2 \mathbf{U}_2^{\mathsf{T}}), \tag{5}$$

$$\implies \frac{\partial \mathcal{L}}{\partial \theta} = 2 e_i^{\top} \mathbf{X}^{\top} \mathbf{X} \mathbf{U}_1 \left(\mathbf{U}_2 \mathbf{U}_2^{\top} \right) e_j.$$
 (6)

Because \mathbf{U}_1 depends linearly on θ only through the i-th row, differentiation once more yields the diagonal Hessian entry

$$\frac{\partial^2 \mathcal{L}}{\partial \theta^2} = 2 e_i^{\top} \mathbf{X}^{\top} \mathbf{X} E_{ij} \mathbf{U}_2 \mathbf{U}_2^{\top} e_j = 2 (\mathbf{X}^{\top} \mathbf{X})_{ii} (\mathbf{U}_2 \mathbf{U}_2^{\top})_{jj}.$$

Letting $\delta\theta=-\theta$ denote the pruning perturbation, a second-order Taylor expansion gives

$$\Delta \mathcal{L}_{ij} = \mathcal{L} \left(\mathbf{U}_{1} + \delta \theta E_{ij} \right) - \mathcal{L} (\mathbf{U}_{1})$$

$$= \underbrace{\frac{\partial \mathcal{L}}{\partial \theta}}_{=0} \delta \theta + \frac{1}{2} \frac{\partial^{2} \mathcal{L}}{\partial \theta^{2}} (\delta \theta)^{2} + O \left(\|\delta \theta\|^{3} \right)$$

$$\approx \frac{1}{2} \theta^{2} (\mathbf{X}^{\top} \mathbf{X})_{ii} (\mathbf{U}_{2} \mathbf{U}_{2}^{\top})_{jj}. \tag{7}$$

Hence, under the stated assumptions, the *exact* second-order approximation to the loss increase is non-negative and is given by

$$\Delta \mathcal{L}_{ij} \approx \frac{1}{2} \theta_{ij}^2 (\mathbf{X}^\top \mathbf{X})_{ii} (\mathbf{U}_2 \mathbf{U}_2^\top)_{jj} \qquad (i \in [d], j \in [h]).$$

This value serves as a principled importance score for weight pruning: the larger the product of the data-covariance entry $(\mathbf{X}^{\top}\mathbf{X})_{ii}$, the downstream energy $(\mathbf{U}_2\mathbf{U}_2^{\top})_{jj}$, and the squared weight magnitude θ_{ij}^2 , the greater the predicted loss incurred by zeroing θ_{ij} .

Training Dataset Construction

The domain training corpora are listed in Tables 3 and 4. For each domain, we stratify the original training split by label, shuffle with a fixed seed (1234), and subsample to the desired size. In PubmedQA, we retain only the *yes* and *no* classes because the released training set contains no *maybe* examples. For all other datasets, labels with too few instances are upsampled by sampling with replacement until the target count is reached. All training data and evaluation scripts follow the Alpaca template (Dubois et al. 2023), with the full prompt formats listed in Appendix .

Table 3: **Health domain** training datasets with label distributions, shuffle settings, random seed, and sequence length.

Dataset	Label	Instances	Shuffle	Seed	Seq. Len.
	entailment	2333	TRUE	1234	2048
MedNLI	contradiction	2333		1234	2048
	neutral	2334		1234	2048
	yes	3500	TRUE	1234	2048
PubMedQA	no	3500		1234	2048
	maybe	0		1234	2048
HQS	_	1000	TRUE	1234	2048

Table 4: **Legal domain** training datasets with label distributions, shuffle settings, random seed, and sequence length.

Dataset	Label	Instances	Shuffle	Seed	Seq. Len.
	entailment	2100	TRUE	1234	2048
ContractNLI	contradiction	1200		1234	2048
	neutral	2700		1234	2048
	0	1400	TRUE	1234	2048
	1	1400		1234	2048
CaseHold	2	1400		1234	2048
	3	1400		1234	2048
	4	1400		1234	2048
BillSum	_	1000	TRUE	1234	2048

Two domain-specific datasets are used in our experiments: **PubMedQA** and **CaseHold**. For **PubMedQA**, we sample 7,000 *yes* and 7,000 *no* examples; the *maybe* label is excluded due to lack of availability in the training split. For **CaseHold**, we sample 3,000 instances from each class label {0, 1, 2, 3, 4}. All dataset splits are shuffled once using a fixed seed

Hyperparameters Settings

We provide all the hyperparameter used for training in Table 1, Table 2, and the two task specific domain model used in Section . For all dense Health domain models, we use training dataset described in Table 3 and the evaluation datasets described in Table 9. For all dense Legal domain models, we use training dataset described in Table 4 and the evaluation datasets described in Table 10. The training hyperparameter are set the be the same for PubMedQA model and CaseHold model with training datasets described

in previous section. To note that all training are conducted on 4 NVIDIA A100 GPUs with 80GB memory. We adjust the per-device batch size and gradient accumulation steps to maintain a global batch size of 32.

Table 5: Dense Health Domain Training Hyperparameters

Hyperparameter	Value
model_name	meta-llama/Llama-2-7b-hf
learning_rate	1×10^{-4}
per_device_batch_size	2
gradient_accumulation_steps	4
num_train_epochs	3
weight_decay	0.01
fp16	True
save_steps	1000
max_seq_length	2048
lora_r	8
lora_alpha	16
lora_dropout	0
lora_bias	none
lora_target_modules	q_proj, o_proj,
lora_target_modules	v_proj,
	k_proj, gate_proj,
	up_proj, down_proj
optimizer	torch_Adam

Table 6: Dense Health Domain Training Hyperparameters

Hyperparameter	Value
model_name	meta-llama/Llama-2-7b-h
learning_rate	1×10^{-4}
per_device_batch_size	2
gradient_accumulation_steps	4
num_train_epochs	3
weight_decay	0.01
fp16	True
save_steps	1000
max_seq_length	2048
lora_r	8
lora_alpha	16
lora_dropout	0
lora_bias	none
lora_target_modules	q_proj, o_proj,
lora_target_modules	v_proj,
	k_proj, gate_proj,
	up_proj, down_proj
optimizer	torch_Adam

The LoRA training hyperparameter and training dataset used for EfficientXpert are identical to those used for the dense model to ensure a fair comparison. For ForeSight Mask, the mask learning rate is set to 0.5. For Partial Brain Surgeon, the regularization coefficient is set to 1×10^{-8} .

Evaluation Details

The name of the evaluation and number of instances in the test set are listed in Table 9 and Table 10. For all the evaluations, we adopt the Alpaca template (Dubois et al. 2023) to evaluate the performance of the models. All Alpaca templates are listed in Appendix .

Table 7: Dense Legal Domain Training Hyperparameters

Hyperparameter	Value
model_name	meta-llama/Llama-2-7b
learning_rate	1×10^{-4}
per_device_batch_size	2
gradient_accumulation_steps	4
num_train_epochs	3
weight_decay	0.01
fp16	True
save_steps	1000
max_seq_length	2048
lora_r	8
lora_alpha	16
lora_dropout	0
lora_bias	none
lore terget modules	q_proj, o_proj,
lora_target_modules	v_proj,
	k_proj, gate_proj,
	up_proj, down_proj
optimizer	torch_Adam

Table 8: Dense Legal Domain Training Hyperparameters

Hyperparameter	Value
model_name	meta-llama/Llama-3-8b
learning_rate	1×10^{-4}
per_device_batch_size	1
gradient_accumulation_steps	8
num_train_epochs	3
weight_decay	0.01
fp16	True
save_steps	1000
max_seq_length	2048
lora_r	8
lora_alpha	16
lora_dropout	0
lora_bias	none
lana tanant mandalan	q_proj, o_proj,
lora_target_modules	v_proj,
	k_proj, gate_proj,
	up_proj, down_proj
optimizer	torch_Adam

Further Analysis

The Grassmann distance between two LoRA adapters of the same weight, parameterized by (B_1, A_1) and (B_2, A_2) respectively, is given by

$$d(U_1, U_2) = \left(\sum_{i=1}^r \cos^{-1}(\sigma_i)^2\right)^{\frac{1}{2}},\tag{8}$$

where
$$B_1 A_1 = U_1 \Sigma_1 V_1^{\top}$$
, $B_2 A_2 = U_2 \Sigma_2 V_2^{\top}$. (9)

and σ_i are the singular values of $U_1^{\top}U_2$, r=8 for our experiment.

To understand how is task information encoded in the LoRA adapter, we further analyze the projection energy of each domain-specific or task-diverse model introduced in Section, as shown in Figure 4. For each model, we compute the projection energy of the LoRA adapters and average it by weight type. The plotted results reveal that the distribution of average projection energy exhibits **more consistent local**

Table 9: Overview of health datasets used for evaluation.

	InternalMed_Harrison	MedNLI	PubMedQA	HQS
Domain	Health	Health	Health	Health
Task / Type	Generation	NLI	QA	Summarization
# Instances in Test	300	1422	500	100
Metrics	Perplexity	Acc & Macro-F1	Acc & Macro-F1	ROUGE

Table 10: Overview of legal datasets used for evaluation.

	MultiLegalPile	ContractNLI	CaseHOLD	BillSum
Domain	Legal	Legal	Legal	Legal
Task / Type	Generation	NLI	QA	Summarization
# Instances in Test	300	1991	200	200
Metrics	Perplexity	Acc & Macro-F1	Acc & Macro-F1	ROUGE

patterns within the same task (e.g., CaseHold vs. Legal or PubMedQA vs. Health), even when the domains differ.

For instance, **PubMedQA** and **Health**, although from different domains, both exhibit strong activation in gate_proj and up_proj. In contrast, **CaseHold** and **Legal** emphasize k_proj and up_proj. This pattern suggests that **task similarity plays a dominant role in shaping local projection energy patterns**, whereas **domain-level information may guide the broader global distribution**. These findings imply that LoRA adapters capture a **global structure governed by domain**, while their **local energy distribution reflects task-specific characteristics**, especially across components like attention, gate, up projection in MLP.

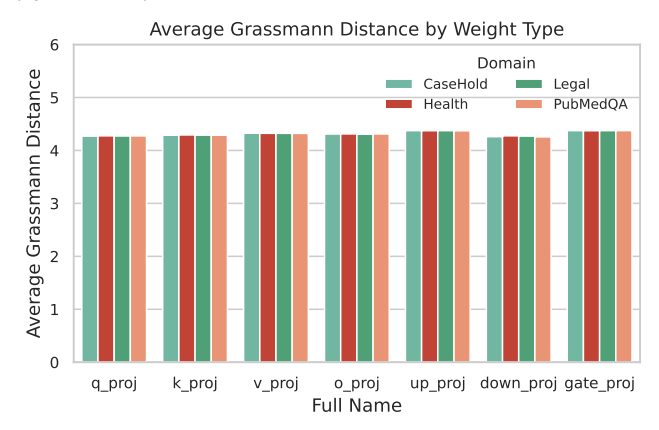


Figure 6: Grassmann distance between LoRA adapters and weight matrices by weight type.

These findings imply that while LoRA adapters may encode a global structure shaped by domain identity, task-specific characteristics drive significant variation in projection energy across weight types—particularly within attention and MLP components.

To further explore this contrast, we visualize the Grassmann distance between LoRA adapters and the corresponding base weight matrices for each layer. As shown in Figure 5, the Grassmann distances remain consistently high (above 4) across all layers and domains, indicating that LoRA adapters systematically amplify directions that diverge from the pretrained model's dominant subspaces. This pattern is mirrored in Figure 6, where all weight types ex-

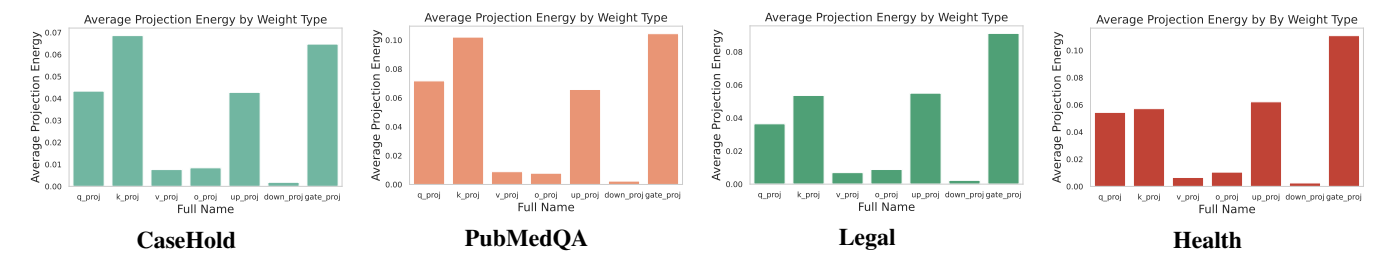


Figure 4: Projection energy by full name across domains.

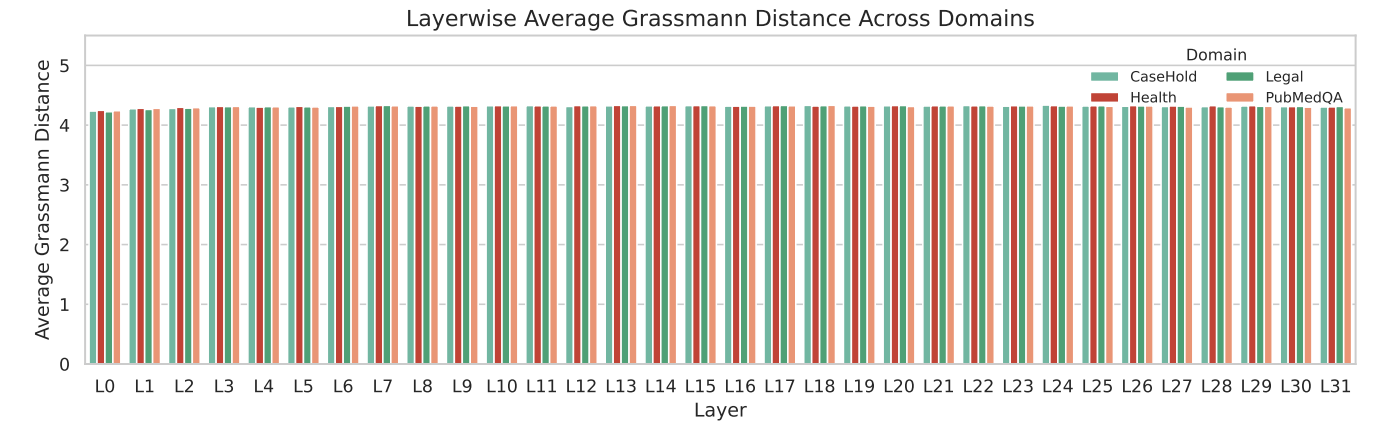


Figure 5: Grassmann distance between LoRA adapters and weight matrices across layers.

hibit similarly large distances.

These results suggest a fundamental duality: while the global subspace shift induced by LoRA is governed by domain-level signals—producing consistently large Grassmann distances—the local alignment revealed by projection energy varies according to task-specific usage patterns.

Alpaca Templates

PubMedQA

- 1 "Below is an instruction that describes a task related to HealthCare, "

- 4 "can you tell me if the following statement is correct? Answer yes, no, or maybe.\n\n"
- 5 "Input:\n"
- 6 "Contexts:\n{contexts}\n\n"
- 7 "Section Labels: {labels}\n\n"
- 8 "MeSH Terms: {meshes}\n\n"
- 9 "Question: {question}\n\n"
- 10 "Response: The answer is"

MedNLI

1 "Below is an instruction for analyzing clinical information. \n "

- 2 "Instruction:\n"
- 3 "You are a licensed physician tasked with determining the logical relationship between two clinical statements based on a patient's past medical history.\n"
- 4 "Analyze carefully whether the second statement (hypothesis) can be inferred from the first statement (premise).\n"
- 5 "Base your reasoning strictly on clinical knowledge, without making unwarranted assumptions.\n"

- 8 "- 'contradiction' if the hypothesis
 must be false given the premise,\n"
- 10 "Fully consider all three possibilities and reason carefully before giving your final answer. \n "
- 12 "Final Answer: Their relationship is {
 gold_label}"

HQS

1 "Below is an instruction that describes

- a task related to HealthCare, paired
 with further context. "
- 2 "Write a response that appropriately completes the request.\n\n"
- 3 "Instruction: Summarize the following consumer health question by generating a condensed version "
- 4 "that retains all critical information necessary to find correct and complete answers. "
- 5 "Focus on preserving key entities (e.g., conditions, treatments, tests) and the main intent of the question, while omitting unnecessary peripheral details."
- 6 "Write the summary fluently in natural language and avoid simply shortening without ensuring information completeness.\n\n"
- 8 "Input: {input_question}\n\nShortened
 Question:"

CaseHold

- 1 "Below is an instruction that describes a task related to making legal decisions based on a citing prompt."
- 2 "Please read the citing prompt, and decide which holding statement best corresponds to it.\n\n"
- 3 "Instruction:\n"
- 4 "You are given a citing passage from a legal decision and five potential holding statements.\n"
- 5 "Your task is to carefully read the citing prompt and select the holding statement that best corresponds to it .\n"
- 6 "Focus on the precise legal principle, factual framing, and implications described.\n"
- 7 "Base your decision purely on the logical match between the citing prompt and the holding, avoiding irrelevant or merely similar content .\n\n"
- 8 "Your answer should be 0, 1, 2, 3, or $4.\n\n$ "
- 9 "Input: citing_prompt: {citing_prompt},
 0: {holding_0}, 1: {holding_1}, 2: {
 holding_2}, 3: {holding_3}, 4: {
 holding_4}\n\n"
- 10 "Response: The answer is"

ContractNLI

- 1 "Below is an instruction that describes a task related to Contracts, paired with an input that provides context.
- 2 "Write a detailed response that includes your reasoning process, then conclude with your final answer.\n\n"

- 3 "Instruction: Carefully analyze the relationship between the Contract Premise and Hypothesis. "
- 5 "Ensure that you fully consider all three relationships.\n\n"
- 6 "Input:\nPremise: '{sentence1}'\
 nHypothesis: '{sentence2}'\n\n"
- 7 "Final Answer: Their relationship is "

BillSum

- 2 "Instruction:\n"
- 3 "Summarize the following legislative
 text by clearly identifying and
 explaining the *major actions,
 purposes, and effects* of the bill."
- 4 "Focus on what the bill aims to achieve rather than technical details or administrative changes."
- 5 "Paraphrase the information in a simple and accessible way as if writing for policymakers and the public."
- 5 "Avoid copying long passages or citing subsection numbers unless necessary for understanding.\n\n"
- 7 "Input:\n"
- 8 "Bill Title: {title}\n\n"
- 9 "{input_text}\n\n"
- 10 "Response:"

Effect of Rank r on Partial Brain Surgeon

When the chosen rank r is substantially smaller than the number of pruned entries $|S_i|$, the resulting system becomes over-constrained, which can degrade downstream performance. To mitigate this, higher sparsity levels generally require a correspondingly larger rank r.

We evaluated the impact of varying r at 50% sparsity on Llama-3.2-1B. As shown in Figure 7, increasing the rank consistently improves relative performance. Each individual metric is recorded in table 11

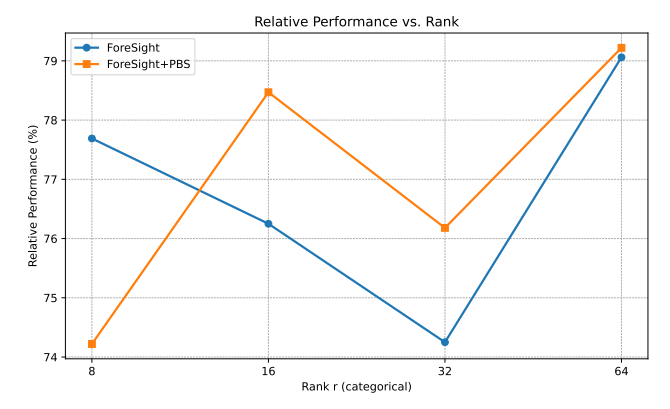


Figure 7: Relative performance of FourSight and FourSight + PBS at 50% sparsity on Llama-3.2-1B.

Table 11: Performance metrics for different methods at various ranks r at 50% sparsity on Llama-3.2-1B.

Method	Rank	Med PPL	MedNLI Acc	MedNLI F1	PubMedQA Acc	PubMedQA F1	HQS R1	HQS R2	HQS RL	Rel%
	8	10.288	0.5605	0.5464	0.6800	0.4714	0.2476	0.0896	0.2204	_
Danca	16	10.145	0.5956	0.5759	0.6600	0.4674	0.2609	0.0852	0.2343	_
Dense	32	10.029	0.6069	0.5986	0.6660	0.4656	0.2507	0.0809	0.2284	_
	64	9.902	0.5872	0.5733	0.6500	0.4575	0.2439	0.0755	0.2122	_
	8	14.716	0.4286	0.3961	0.5200	0.3710	0.2171	0.0688	0.1948	77.69
01140	16	14.706	0.4286	0.3961	0.5200	0.3710	0.2171	0.0688	0.1948	76.26
ours	32	14.685	0.4197	0.3620	0.5205	0.3716	0.2114	0.0672	0.1914	74.26
	64	14.834	0.3926	0.3921	0.5300	0.3972	0.2201	0.0693	0.1974	79.06
	8	15.854	0.3643	0.3412	0.5720	0.4027	0.1960	0.0568	0.1757	74.22
oursPBS	16	15.020	0.4365	0.4252	0.5395	0.3845	0.2206	0.0637	0.1980	78.47
	32	14.908	0.3968	0.3979	0.5505	0.3917	0.2117	0.0641	0.1894	76.18
	64	15.106	0.3954	0.3824	0.5490	0.3910	0.2227	0.0688	0.1998	79.22

Discuss on the Artifacts

The license for the models and datasets used in this paper is as follows:

- Llama-2-7b-hf: The model is licensed under the LLaMA 2 community license.
- Llama-3-8b: The model is licensed under META LLaMA 3 community license.
- PubMedQA: The dataset is licensed under MIT license.
- **MedNLI**: The dataset is licensed under the Physionet Credentialed Health Data License Version 1.5.0.
- **HQS**: The dataset is licensed under Apache License 2.0.
- CaseHold: The dataset is licensed under Apache License 2.0
- ContractNLI: The dataset is licensed under the CC BY 4.0 license.

References

An, Y.; Zhao, X.; Yu, T.; Tang, M.; and Wang, J. 2025. Systematic outliers in large language models. *arXiv preprint arXiv:2502.06415*.

Anil, R.; Dai, A. M.; Firat, O.; Johnson, M.; Lepikhin, D.; Passos, A.; Shakeri, S.; Taropa, E.; Bailey, P.; Chen, Z.; et al. 2023. Palm 2 technical report. *arXiv preprint arXiv:2305.10403*.

Bandari, A.; Yin, L.; Hsieh, C.-Y.; Jaiswal, A. K.; Chen, T.; Shen, L.; Krishna, R.; and Liu, S. 2024. Is c4 dataset optimal for pruning? an investigation of calibration data for llm pruning. *arXiv* preprint arXiv:2410.07461.

Bhattacharyya, C.; and Kim, Y. 2025. FineScope: Precision Pruning for Domain-Specialized Large Language Models Using SAE-Guided Self-Data Cultivation. *arXiv* preprint *arXiv*:2505.00624.

Cheng, H.; Zhang, M.; and Shi, J. Q. 2024. A survey on deep neural network pruning: Taxonomy, comparison, analysis, and recommendations. *IEEE Transactions on Pattern Analysis and Machine Intelligence*.

Dubey, A.; Jauhri, A.; Pandey, A.; Kadian, A.; Al-Dahle, A.; Letman, A.; Mathur, A.; Schelten, A.; Yang, A.; Fan, A.; et al. 2024. The llama 3 herd of models. *arXiv e-prints*, arXiv–2407.

Dubois, Y.; Li, C. X.; Taori, R.; Zhang, T.; Gulrajani, I.; Ba, J.; Guestrin, C.; Liang, P. S.; and Hashimoto, T. B. 2023. Alpacafarm: A simulation framework for methods that learn from human feedback. *Advances in Neural Information Processing Systems*, 36: 30039–30069.

Frantar, E.; and Alistarh, D. 2023. Sparsegpt: Massive language models can be accurately pruned in one-shot. In *International conference on machine learning*, 10323–10337. PMLR.

Guo, H.; Gao, J.; and Yuan, Y. 2025. Enhancing Low-Rank Adaptation with Recoverability-Based Reinforcement Pruning for Object Counting. In *Proceedings of the AAAI Conference on Artificial Intelligence*, volume 39, 3238–3246.

Han, S.; Mao, H.; and Dally, W. J. 2015. Deep compression: Compressing deep neural networks with pruning,

- trained quantization and huffman coding. arXiv preprint arXiv:1510.00149.
- Hu, E. J.; Shen, Y.; Wallis, P.; Allen-Zhu, Z.; Li, Y.; Wang, S.; Wang, L.; Chen, W.; et al. 2022. Lora: Low-rank adaptation of large language models. *ICLR*, 1(2): 3.
- Ji, Y.; Xiang, Y.; Li, J.; Xia, Q.; Li, P.; Duan, X.; Wang, Z.; and Zhang, M. 2024. Beware of calibration data for pruning large language models. *arXiv* preprint arXiv:2410.17711.
- Jin, Q.; Dhingra, B.; Liu, Z.; Cohen, W. W.; and Lu, X. 2019. Pubmedqa: A dataset for biomedical research question answering. *arXiv* preprint arXiv:1909.06146.
- Kuznedelev, D.; Tabesh, S.; Noorbakhsh, K.; Frantar, E.; Beery, S.; Kurtic, E.; and Alistarh, D. 2023. Vision models can be efficiently specialized via few-shot task-aware compression. *arXiv preprint arXiv:2303.14409*.
- Li, X. L.; and Liang, P. 2021. Prefix-tuning: Optimizing continuous prompts for generation. *arXiv preprint arXiv:2101.00190*.
- Lu, L.; Wang, Z.; Bao, R.; Wang, M.; Li, F.; Wu, Y.; Jiang, W.; Xu, J.; Wang, Y.; and Gao, S. 2024. All-in-one tuning and structural pruning for domain-specific llms. *arXiv* preprint *arXiv*:2412.14426.
- Mitra, P.; Schwalbe, G.; and Klein, N. 2024. Investigating calibration and corruption robustness of post-hoc pruned perception cnns: An image classification benchmark study. In *Proceedings of the IEEE/CVF Conference on Computer Vision and Pattern Recognition*, 3542–3552.
- Park, S.; Lee, J.; Mo, S.; and Shin, J. 2020. Lookahead: A far-sighted alternative of magnitude-based pruning. *arXiv* preprint arXiv:2002.04809.
- Qin, Z.; Yu, F.; Liu, C.; and Chen, X. 2018. How convolutional neural network see the world-A survey of convolutional neural network visualization methods. *arXiv* preprint *arXiv*:1804.11191.
- Romanov, A.; and Shivade, C. 2018. Lessons from natural language inference in the clinical domain. *arXiv preprint arXiv:1808.06752*.
- Song, Z.; Yan, B.; Liu, Y.; Fang, M.; Li, M.; Yan, R.; and Chen, X. 2025. Injecting domain-specific knowledge into large language models: a comprehensive survey. *arXiv* preprint arXiv:2502.10708.
- Sun, M.; Chen, X.; Kolter, J. Z.; and Liu, Z. 2024. Massive activations in large language models. *arXiv preprint arXiv:2402.17762*.
- Sun, M.; Liu, Z.; Bair, A.; and Kolter, J. Z. 2023. A simple and effective pruning approach for large language models. *arXiv* preprint arXiv:2306.11695.
- Touvron, H.; Martin, L.; Stone, K.; Albert, P.; Almahairi, A.; Babaei, Y.; Bashlykov, N.; Batra, S.; Bhargava, P.; Bhosale, S.; et al. 2023. Llama 2: Open foundation and fine-tuned chat models. *arXiv preprint arXiv:2307.09288*.
- Williams, M.; and Aletras, N. 2023. On the impact of calibration data in post-training quantization and pruning. *arXiv* preprint arXiv:2311.09755.

- Wu, D.; Guo, Z.; Yu, L.; Sang, N.; and Gao, C. 2025. Structural Pruning via Spatial-aware Information Redundancy for Semantic Segmentation. In *Proceedings of the AAAI Conference on Artificial Intelligence*, volume 39, 8368–8376.
- Wu, Z.; Chen, J.; and Wang, Y. 2025. Unified knowledge maintenance pruning and progressive recovery with weight recalling for large vision-language models. In *Proceedings of the AAAI Conference on Artificial Intelligence*, volume 39, 8550–8558.
- Yang, H.; Liu, X.-Y.; and Wang, C. D. 2023. Fingpt: Open-source financial large language models. arXiv. arXiv preprint arXiv:2306.06031.
- Zhang, J.; Wang, J.; Li, H.; Shou, L.; Chen, K.; You, Y.; Xie, G.; Gong, X.; and Zhou, K. 2025. Train small, infer large: Memory-efficient lora training for large language models. *arXiv preprint arXiv:2502.13533*.
- Zhang, M.; Chen, H.; Shen, C.; Yang, Z.; Ou, L.; Yu, X.; and Zhuang, B. 2023. Loraprune: Pruning meets low-rank parameter-efficient fine-tuning. *ICLR*.
- Zhang, N.; Liu, Y.; Zhao, X.; Cheng, W.; Bao, R.; Zhang, R.; Mitra, P.; and Chen, H. 2024. Pruning as a domain-specific llm extractor. *arXiv preprint arXiv:2405.06275*.
- Zheng, L.; Guha, N.; Anderson, B. R.; Henderson, P.; and Ho, D. E. 2021. When does pretraining help? assessing self-supervised learning for law and the casehold dataset of 53,000+ legal holdings. In *Proceedings of the eighteenth international conference on artificial intelligence and law*, 159–168.
- Zhou, Z.; Shi, J.-X.; Song, P.-X.; Yang, X.-W.; Jin, Y.-X.; Guo, L.-Z.; and Li, Y.-F. 2024. Lawgpt: A chinese legal knowledge-enhanced large language model. *arXiv preprint arXiv:2406.04614*.

Reproducibility Checklist

Instructions for Authors:

This document outlines key aspects for assessing reproducibility. Please provide your input by editing this .tex file directly.

For each question (that applies), replace the "Type your response here" text with your answer.

Example: If a question appears as

\question{Proofs of all novel claims
are included} {(yes/partial/no)}
Type your response here

you would change it to:

\question{Proofs of all novel claims
are included} {(yes/partial/no)}
ves

Please make sure to:

- Replace ONLY the "Type your response here" text and nothing else.
- Use one of the options listed for that question (e.g., yes, no, partial, or NA).
- Not modify any other part of the \question command or any other lines in this document.

You can \input this .tex file right before \end{document} of your main file or compile it as a stand-alone document. Check the instructions on your conference's website to see if you will be asked to provide this checklist with your paper or separately.

1. General Paper Structure

- 1.1. Includes a conceptual outline and/or pseudocode description of AI methods introduced (yes/partial/no/NA) yes
- 1.2. Clearly delineates statements that are opinions, hypothesis, and speculation from objective facts and results (yes/no) yes
- 1.3. Provides well-marked pedagogical references for less-familiar readers to gain background necessary to replicate the paper (yes/no) yes

2. Theoretical Contributions

2.1. Does this paper make theoretical contributions? (yes/no) yes

If yes, please address the following points:

- 2.2. All assumptions and restrictions are stated clearly and formally (yes/partial/no) yes
- 2.3. All novel claims are stated formally (e.g., in theorem statements) (yes/partial/no) **yes**

- 2.4. Proofs of all novel claims are included (yes/partial/no) yes
- 2.5. Proof sketches or intuitions are given for complex and/or novel results (yes/partial/no) yes
- 2.6. Appropriate citations to theoretical tools used are given (yes/partial/no) yes
- 2.7. All theoretical claims are demonstrated empirically to hold (yes/partial/no/NA) yes
- 2.8. All experimental code used to eliminate or disprove claims is included (yes/no/NA) yes

3. Dataset Usage

3.1. Does this paper rely on one or more datasets? (yes/no) **ves**

If yes, please address the following points:

- 3.2. A motivation is given for why the experiments are conducted on the selected datasets (yes/partial/no/NA) yes
- 3.3. All novel datasets introduced in this paper are included in a data appendix (yes/partial/no/NA) yes
- 3.4. All novel datasets introduced in this paper will be made publicly available upon publication of the paper with a license that allows free usage for research purposes (yes/partial/no/NA) yes
- 3.5. All datasets drawn from the existing literature (potentially including authors' own previously published work) are accompanied by appropriate citations (yes/no/NA) yes
- 3.6. All datasets drawn from the existing literature (potentially including authors' own previously published work) are publicly available (yes/partial/no/NA) yes
- 3.7. All datasets that are not publicly available are described in detail, with explanation why publicly available alternatives are not scientifically satisficing (yes/partial/no/NA) yes

4. Computational Experiments

4.1. Does this paper include computational experiments? (yes/no) yes

If yes, please address the following points:

- 4.2. This paper states the number and range of values tried per (hyper-) parameter during development of the paper, along with the criterion used for selecting the final parameter setting (yes/partial/no/NA) yes
- 4.3. Any code required for pre-processing data is included in the appendix (yes/partial/no) yes

- 4.4. All source code required for conducting and analyzing the experiments is included in a code appendix (yes/partial/no) yes
- 4.5. All source code required for conducting and analyzing the experiments will be made publicly available upon publication of the paper with a license that allows free usage for research purposes (yes/partial/no) yes
- 4.6. All source code implementing new methods have comments detailing the implementation, with references to the paper where each step comes from (yes/partial/no) yes
- 4.7. If an algorithm depends on randomness, then the method used for setting seeds is described in a way sufficient to allow replication of results (yes/partial/no/NA) yes
- 4.8. This paper specifies the computing infrastructure used for running experiments (hardware and software), including GPU/CPU models; amount of memory; operating system; names and versions of relevant software libraries and frameworks (yes/partial/no) yes
- 4.9. This paper formally describes evaluation metrics used and explains the motivation for choosing these metrics (yes/partial/no) yes
- 4.10. This paper states the number of algorithm runs used to compute each reported result (yes/no) yes
- 4.11. Analysis of experiments goes beyond single-dimensional summaries of performance (e.g., average; median) to include measures of variation, confidence, or other distributional information (yes/no) yes
- 4.12. The significance of any improvement or decrease in performance is judged using appropriate statistical tests (e.g., Wilcoxon signed-rank) (yes/partial/no) partial
- 4.13. This paper lists all final (hyper-)parameters used for each model/algorithm in the paper's experiments (yes/partial/no/NA) yes